Water Science & Technology

Water Science & Technology Vol 87 No 9, 2210 doi: 10.2166/wst.2023.128

Optimization of thermal–alkaline pretreatment for dewatering of excess sludge followed by thermal/persulfate oxidation for the elimination of extracellular ARGs in TAP-treated filtrate

Pengcheng Yao and Aiju You*

Zhejiang Institute of Hydraulics and Estuary (Zhejiang Institute of Marine Planning and Design), Hangzhou, Zhejiang 310000, China
*Corresponding author. E-mail: 0622793@zju.edu.cn

ABSTRACT

This study evaluated the dewatering of excess sludge and the removal of extracellular antibiotic-resistant genes (eARGs) from the treated filtrate by thermal–alkaline pretreatment (TAP) and thermal/persulfate (PS). The optimization of TAP and thermal/PS was investigated during excess sludge dewatering and removal of eARGs via response surface methodology (RSM). The results demonstrated that TAP could effectively decrease the water content of excess sludge (41%) at optimum operating conditions (such as temperature: 88 °C, operation time: 90 min, pH: 11.2). However, the increase in eARGs abundance in TAP-treated filtrate is probably due to the dissolved effluent of the intracellular matter during dewatering. Therefore, TAP-treated filtrate was subjected to thermal/PS, and the removal of eARGs after TAP was explored. The desirability function was used to optimize two kinds of removal efficiencies of eARGs, simultaneously. The optimal pH, persulfate concentration, and reaction temperature were 10.2, 0.039 M, and 75.12 °C, respectively. 6.28 log·copies/mL of *tetA* and 6.57 log·copies/mL of *sulI* were removed under the above-mentioned conditions. The process provided efficient dewatering of excess sludge and elimination of eARGs from the filtrate.

Key words: alkaline, dewatering, excess sludge, extracellular antibiotic-resistant genes, thermal

HIGHLIGHTS

- TAP significantly enhanced the sludge dewatering efficiency.
- The abundance of eARGs increases significantly after TAP.
- The desirability function was used to optimize multiple target parameters.
- Thermal/PS can effectively reduce the abundance of eARGs, even below the detection limit.

GRAPHICAL ABSTRACT

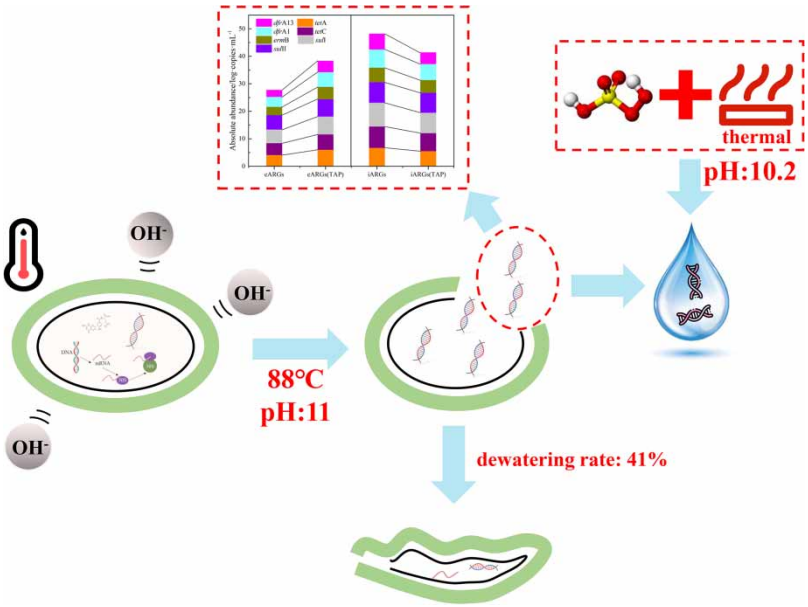

1. INTRODUCTION

At present, the main process of most wastewater treatment plants (WWTPs) is biological treatment, especially the activated sludge process or its modified processes. However, excess sludge is a by-product of biological treatment processes that take place in WWTPs (Mancuso *et al.* 2019). It was estimated that municipal sludge production in China reached 40 million tons in 2019 (Wei *et al.* 2020). Excess sludge contains high-risk pollutants that require proper and safe disposal. In general, sludge treatments can be summarized as disposal (land-fillings and incineration) and reuse (soil remediation). Among them, sludge dewatering is the essential step in excess sludge treatment. According to the landfill standard in China, the water content of sludge needed to be decreased to 60% (Zhang *et al.* 2020). After the untreated excess sludge was dewatered via a sludge dehydrator, the water content drops to 70–80%, which cannot meet the landfill standard. Therefore, it is necessary to further treat the excess sludge to achieve dewatering efficiency.

Thermal–alkaline pretreatment (TAP) is a common technique for excess sludge treatment, improving the rate of dewatering of excess sludge (Zhong *et al.* 2015). TAP could avoid operational risks effectively due to high-temperature conditions. Due to the synergistic effects of thermal and alkaline conditions, TAP (<100 °C) requires less energy demand than other high-temperature pretreatment technology (Guo *et al.* 2017). The TAP uses bases such as NaOH, $Ca(OH)_2$, KOH, and NH_3H_2O, and NaOH is the most common base used in alkaline pretreatment. NaOH loadings are normally applied in the range of 1–10% g/g (Zheng *et al.* 2014). TAP could change the cellulosic crystal structure to destroy the ester bonds of lignin–carbohydrate complexes (Tsapekos *et al.* 2016). Moreover, the disintegration of extracellular polymeric substances (EPSs) and cell walls are recognized as the key limitations to efficient dewatering (Duan *et al.* 2020). TAP can also destroy cells wall and EPSs, resulting in the release of intracellular water and water combined with EPSs (Guo *et al.* 2017). However, one major constraint of this process is the significant increase of extracellular antibiotic-resistant genes (eARGs) in the effluent, which may cause a huge potential risk to receiving environment.

ARGs raise serious concern for public health as an important contaminant of emerging concern (CEC) (Pruden *et al.* 2006). The CECs are associated with an identified harmful health and environmental impact, even though they are present in trace amounts in the environment (Khan *et al.* 2022). Bacteria can acquire ARGs via horizontal gene transfer (HGT), which can be summarized by conjugation, transduction, and transformation (Lu *et al.* 2020a). A high abundance of eARGs remained in the sludge filtrate after the dewatering process, which could disseminate among the microbial community through the transformation of HGT frequently (Blokesch 2016). The excess sludge is not disposed of properly, which will bring huge pressure to the transfer of ARGs in the receiving environment.

Advanced chemical oxidation processes (AOPs) were used as a powerful source of reactive radicals to treat intracellular ARGs (Michael-Kordatou *et al.* 2018) and extracellular ARGs (Krzeminski *et al.* 2020). Among them, persulfate (PS) is the common oxidant, which has a high oxidizing ability (Ran & Li 2020). The oxidant is activated to produce highly reactive radical species, such as hydroxyl radical and sulfate radical (Hilles *et al.* 2016). Also, the high temperature is an effective way to activate reactive radical species (Su *et al.* 2019). The optimization of the TAP and thermal/PS was studied (Campo *et al.* 2018; Pourehie & Saien 2019). Compared with the conventional optimization method, response surface methodology (RSM) needs fewer experiments to optimize the process parameters (Xie *et al.* 2016).

Four objectives of this study were as follows: (a) to investigate the efficiency of TAP in dewatering from excess sludge, (b) to investigate the impact of TAP on eARGs, (c) to explore the degradation efficiency of eARGs by thermal/PS (AOP), and (d) to determine the optimal reaction condition of the TAP and thermal/PS via RSM. This study may contribute to understand the optimal dewatering process condition and the fate of eARGs during excess sludge dewatering, which also provides guidance for the application of TAP for dewatering rate and thermal/PS process for the removal of eARGs.

2. MATERIALS AND METHODS

2.1. Collection of samples

The sludge was obtained from the biological reaction tank of a reclaimed water reuse system (RWRS) (Supplementary material, Figure S1). The biological treatment process of the RWRS was an anoxic–membrane bioreactor (MBR). The capacity of the RWRS was 1,200 m^3/day, and the hydraulic retention time of the anoxic tank and MBR tank was 3 and 7 h. The sludge had a solid concentration of 9,200–11,200 mg/L. The sludge samples were stored in pre-cleaned aluminum boxes, brought to the laboratory, and stored at −20 °C.

2.2. Optimization of TAP conditions and determination of moisture content

Excess sludge was heated in an electric heater in a 1-L tank until the desired temperature is reached. The sludge was added to the NaOH solution (20 g/L) until reaching the desired pH (10, 11, 12) and stirred by a blender. NaOH is widely used in chemical experiments, and has the commonness of alkali. Also, it can react with a variety of acids and organic matter. RSM was performed to optimize the experimental conditions.

Moisture content (ω) was measured by a funnel with a quantitative filter paper and oven drying. The sample with a weight of m was drained through a weighing filter paper with a constant weight of m_1 in the funnel. Also, the sample was dried in an oven at 105 °C for 2 h until maintaining a constant weight of m_2. The formula for the dewatering rate was as follows:

$$\omega = \frac{m - (m_2 - m_1)}{m} \times 100\% \tag{1}$$

To clarify the degree of sludge cracking, the degree of sludge cracking (DC) could be calculated as follows (Penghe *et al.* 2020):

$$DC = \frac{\rho(SCOD_{TAP}) - \rho(SCOD_0)}{\rho(TCOD_0) - \rho(SCOD_0)} \times 100\% \tag{2}$$

where $\rho(SCOD_{TAP})$ was the TAP-treated dissolved COD, $\rho(SCOD_0)$ was the initial dissolved COD, and $\rho(TCOD_0)$ was the total COD in the sludge.

2.3. Optimization of thermal/PS conditions

Excess sludge was treated by AOPs in a reactor of height 450 mm and diameter 400 mm (Supplementary material, Figure S2). The reaction temperature was maintained at specified temperatures (70, 80, and 90 °C). A 1,000 mL of the supernatant sample with different concentrations of PS (0.02, 0.03, and 0.04 M) under different conditions was injected into the reactor and mixed using a magnetic stirrer at 500 rpm. The important impact factors of the experiment were the initial solution pH, the concentration of PS, and reaction temperature (Furman *et al.* 2010; Asaithambi *et al.* 2017). Therefore, these three parameters were selected as independent variables and the removal efficiency of ARGs was selected as the dependent variable.

2.4. DNA extraction and quantitative polymerase chain reaction

All samples were placed in a refrigerator at 4 °C and the supernatant was collected. The residual solid and cells were removed from the supernatant by filtering through a 0.22 μm membrane. The extracted DNA in the filtrate was collected by precipitation (Zhang *et al.* 2018). Three hundred thirty millilitres (330 mL) of filtrate was added to a mixed solution containing 726 mL of absolute ethanol and 33 mL of 3 M sodium acetate solution, and the mixed solution was placed in a refrigerator at −20 °C for more than 12 h to precipitate the extracellular free DNA. The precipitates were obtained by centrifuging at 10,000 × *g* for 10 min and the supernatants were discarded, followed by air drying for 10 min. DNA extraction from dry precipitates was done according to the method followed by PowerSoil DNA Isolation Kit (Mo Bio, USA). The concentration of the extracted DNA was examined using NanoDrop 2000 (Thermo Fisher, USA).

Quantitative determination of target genes used the SYBR Green I method by a real-time PCR instrument (Bio-Rad CFX96 Touch, USA). The volume of the qPCR mixture was 20 μL, including 10 μL of SYBR Premix Ex Taq (Takara, Dalian, China), 2 μL of template DNA, 0.4 μL of each primer, and 7.2 μL of ddH_2O. The primers for the ARGs quantification are listed in Supplementary material, Table S1. The reaction procedure was divided into pre-denaturation, denaturation, annealing, and extension. Standard curves were constructed based on the past research (Zhang *et al.* 2018). The standard plasmid was diluted in a 10-fold gradient. The correlation coefficients of the standard curves in this study were all >0.99 with the amplification efficiencies of 85–110% (Bai *et al.* 2012). All samples in the qPCR analysis were performed in triplicate.

2.5. Experiment design and data analysis

The treated supernatant was subjected to advanced oxidation to achieve the efficient removal of ARGs in the sludge. The experiment was optimized by the RSM in Box–Behnken Design (BBD), which was an effective technique to analyze experiments, and interpreted by the analysis of variance (ANOVA) (Xie *et al.* 2016). Due to the fitting error of the RSM experiment, data were evaluated by ANOVA to verify the significance of the particular model (Yusup *et al.* 2014).

In the designed experiment, three parameters were selected as the independent variables in the TAP-thermal/PS and the dewatering rate of sludge and removal efficiency of *tetA* and *sulI* were selected as their responses. The range and levels of the independent variables determined in the experiments are given in Supplementary material, Table S2.

The second-order model which shows the relationship of the response variable (y) and predictor variables (x_1, x_2, …, x_i) is

$$y = \alpha_0 + \sum_{i=1}^{n} \alpha_i x_i + \sum_{i=1}^{n} \alpha_{ii} x_i^2 + \sum_{i=1}^{n} \sum_{j=1}^{j<i} \alpha_{ij} x_i x_j \tag{3}$$

where α_i, α_{ii}, α_{ij}, $i, j = 1, 2, \ldots, n$, are the linear parameters, quadratic parameters, and interactive parameters, respectively (Zhu *et al.* 2011).

In general, there were three types of methods to evaluate the significance and reliability of the model. Firstly, the P and F values indicate the influencing items on the response (Inayat *et al.* 2020). Secondly, the regression coefficients (R^2) imply the reliability of predicted values (Shahbaz *et al.* 2017). Thirdly, the lack of fit shows the systematic error (Raheem *et al.* 2018).

2.6. Establishment of desirability function

The desirability function was used for optimizing two kinds of removal efficiencies of eARGs simultaneously (Bezerra *et al.* 2019). The method based on the desirability functions can adjust different parameters so that various optimization standards can be established to achieve the best conditions. In brief, each response was transformed into a dimensionless individual desirability (d_i), and the transformation function is presented in the following equation.

$$d = \begin{cases} 0 & \text{if } y_i < L_i \\ \left(\dfrac{y_i - L_i}{U_i - L_i}\right)^s & \text{if } L_i \le y_i \le U_i \\ 1 & \text{if } y_i > U_i \end{cases} \tag{4}$$

where y_i was the broken efficiency or removal efficiency of each response, L_i was the completely undesirable broken efficiency or removal efficiency, U_i was the desirable broken efficiency or removal efficiency. s was a parameter, in general, $s = 2$ was chosen (Li & Liu 2015).

With the individual desirability, the overall desirability was obtained (D). The overall desirability function D was the weighted geometric mean of the individual desirability (Equation (5)).

$$D = (d_1^{r1} \times d_2^{r2} \times \ldots d_n^{rn})^{1/n} \tag{5}$$

where r_i was a parameter that expresses the importance of each variable.

3. RESULTS AND DISCUSSION

3.1. Analysis of variance

Supplementary material, Table S3 shows the BBD with three factors in three levels, the experimental and predicted results of TAP and thermal/PS. Three important process variables were evaluated for the dewatering rate (pH, temperature, and time) and removal efficiency of eARGs (pH, concentration, and temperature) in TAP and thermal/PS. The data show that the predicted value is in good agreement with the experimental value.

The regression analysis of two process variables was carried out. The values of coefficients and the significance levels are shown in Supplementary material, Table S4. It could be seen that, for the TAP, the linear coefficients of reaction time (α_3), temperature (α_2), and the interaction coefficient of pH with reaction time (α_{13}) as well as the quadratic coefficients α_{22} were significant for the dewatering rate at a level of less than 5%. For the thermal/PS to remove *tetA*, the linear coefficients α_1,the interaction coefficient α_{13}, and the quadratic coefficients α_{22}, α_{33} were the significant variables. For the thermal/PS to remove *sulI*, the linear coefficients α_1,the interaction coefficient α_{13}, and the quadratic coefficients α_{11} were the significant variables. The result indicated that significant parameters affect the removal efficiency of ARGs.

On the basis of the coefficients in Supplementary material, Table S4, the dewatering rate and the removal efficiencies of eARGs could be explained by independent variables. Also, the models are as follows:

(a) dewatering rate by TAP

$$Y(\%) = -1803.10 + 211.44X_1 + 12.45X_2 + 3.82X_3 - 0.32X_1X_2 - 0.20X_1X_3 - 0.0055X_2X_3 - 7.70X_1^2 - 0.05X_2^2 - 0.007X_3^2$$

(b) removal efficiency of *tetA* by thermal/PS

$$Y(log) = 2.38 + 0.09X_1 + 0.02X_2 + 184.26X_3 + 0.000227X_1X_2 - 4.68X_1X_3 + 0.02X_2X_3 + 0.0074X_1^2 + 0.000143X_2^2 - 2339.35X_3^2$$

(c) removal efficiency of *sulI* by thermal/PS

$$Y(log) = 4.44 - 0.13X_1 + 2.75X_2 + 80.88X_3 + 0.000923X_1X_2 - 10.19X_1X_3 + 0.08X_2X_3 + 0.02X_1^2 - 0.0000998X_2^2 - 96.56X_3^2$$

where X_1, X_2, and X_3 are the coded parameters of the independent variables (Supplementary material, Table S2).

The data show that the predicted value is in good agreement with the experimental value.

To certify that the model will be suitable for the experimental data, it was necessary to test whether the model shows significant regression or a non-significant lack of fits (Bezerra *et al.* 2008). There were three types of methods to evaluate the significance of the models. The '*P*-value' of 0.0001, 0.0039, and 0.0058 imply a good correlation between the models. The three models have high regression coefficients ($R^2 = 0.9823$, 0.9227, and 0.9122, respectively) as shown in Supplementary material, Table S5, which implies that up to 91.22% of the variations for dewatering rate and removal efficiency of eARGs could be explained by the independent variables. The 'Lack of Fit' *P*-value of 9.73–36.66% suggests that there was only 9.73–36.66% chance that a 'Lack of Fit' of this large could occur due to noise. All those data indicated that those three models were of great significance and were suitable for fitting the relationship between the dewatering rate or removal efficiencies of eARGs and the three independent variables.

3.2. Application of TAP for dewatering

3.2.1. Determination of the TAP optimal conditions

Figure 1 shows the effects of two variables on the dewatering rate, while the other variables remained at the zero level (Supplementary material, Table S2). It also indicated that the effect of temperature changes on the dewatering rate was more important than others. The dewatering rate increased with time and pH increase. Among them, the influence of temperature is more significant than others, and the dewatering rate increased from 29.91 to 40.53% with the temperature increase. The optimum process parameters (pH: 11.2, temperature: 88 °C, time: 90 min) were obtained and the dewatering rate was 41% for the TAP. The result was consistent with the previous report (Li *et al.* 2017).

The water of the sludge included intracellular water and water with combined polymeric substances (EPSs). From these results, the cell wall structure of the bacteria was destroyed by TAP and it increased the release of intracellular water and organic matter. TAP technology can destruct the structure of EPSs to release cell-associated water. Moreover, the cell wall can be destroyed more easily with high temperatures (Li *et al.* 2017). The addition of alkali caused accelerated decomposition of the cell walls. At high pH values, solubilization of EPSs leads to several reactions in the cell wall to release intracellular water (Toutian *et al.* 2020a). The orthophosphate bonds of phospholipids in the cell wall were easily destroyed at the combined conditions of thermal and alkali (Toutian *et al.* 2020b). The dewatering rate by combined thermal–alkaline was higher than the simple thermal treatment (Li *et al.* 2012).

3.2.2. The relationship between the dewatering rate and the degree of sludge cracking

TAP could rupture the cell and convert some matter from the intracellular state to the extracellular state, and the content of organic matter in the filtrate increases accordingly. It could be seen from Supplementary material, Figure S3(a) that the soluble chemical oxygen demand (*SCOD*) in the untreated sludge is 120 mg/L. Under TAP optimum conditions, *SCOD* increases from 120 mg/L in the initial state to 3,320 mg/L at 100 min.

The previous study showed that the dewatering rate was significantly related to the degree of sludge cracking. The *SCOD* could reflect the degree of sludge cracking, and the degree of sludge cracking can be calculated by Equation (2). As was shown in Supplementary material, Figure S3(b), the sludge dewatering increases with the degree of sludge cracking from 20 to 80 min under optimum conditions of TAP. But the trend of sludge dewatering was opposite to the degree of sludge cracking from 80 to 100 min. The dewatering rate reached 40.14% at 80 min. These results suggest that sludge cracking played a crucial role in dewatering. Guo *et al.* (2017) reported that TAP was helpful for sludge cracking, and it was an effective method for dewatering of sludge. With the cell wall being ruptured, EPS accumulated in the sludge, which leads to a

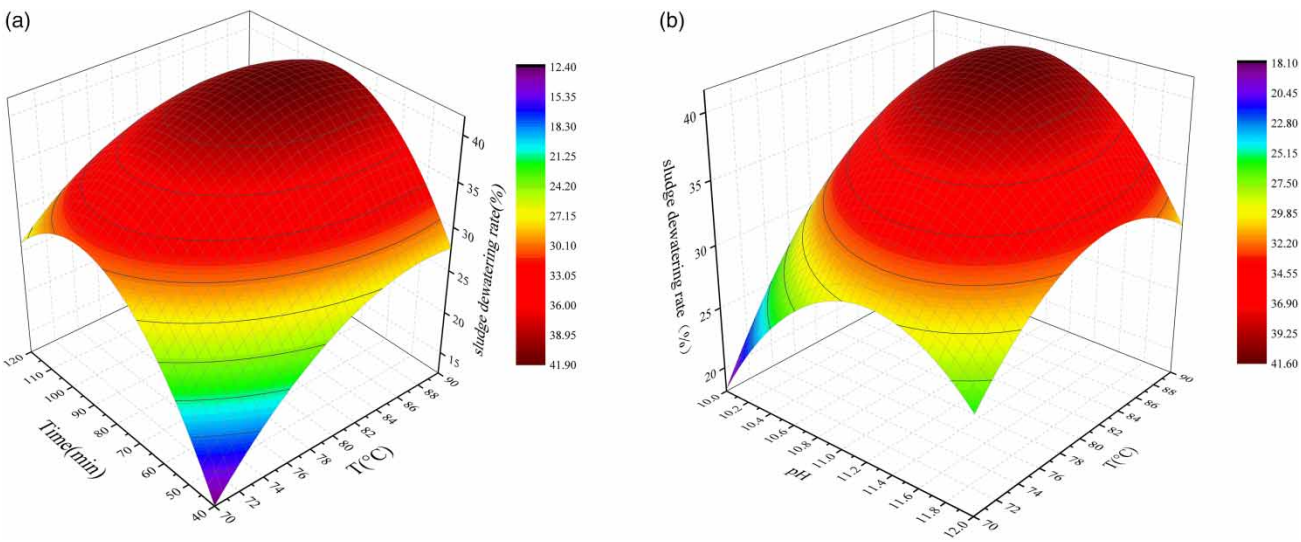

Figure 1 | Three-dimensional surface plots of the experimental data of dewatering rate with two shown variables (other variable not shown in the figure remains at the zero level). (a) Three-dimensional surface plots of the experimental data of dewatering rate with time and temperature. (b) Three-dimensional surface plots of the experimental data of dewatering rate with pH and temperature.

dewatering capacity decrease. It was found that the degree of sludge cracking was useful for sludge dewatering (Ruiz-Hernando *et al.* 2014), but massive sludge cracking also had negative effects on sludge dewatering (Lu *et al.* 2019).

3.2.3. The fate of eARGs and iARGs during TAP

Figure 2(a) shows that the absolute abundances of the tested seven eARGs and iARGs in the raw sludge were $10^{2.37}$–$10^{5.21}$ and $10^{5.30}$–$10^{8.64}$ copies/mL, respectively. Conditioning of the sludge using TAP significantly increases the absolute abundances of eARGs by 1.06–1.90 log copies and reduced the absolute abundances of iARGs by 0.21–1.43 log copies, respectively. A previous study revealed that sludge with ZVI/$S_2O_8^{2-}$ reduced the abundance of iARGs effectively, but eARGs were accumulated in sludge (Lu *et al.* 2020b). Figure 2(b) shows that the absolute abundances of the intracellular and extracellular *intI*1 in the raw sludge were $10^{8.44}$, $10^{5.00}$ copies/mL and 16S rDNA were $10^{10.46}$, $10^{6.16}$ copies/mL. After TAP treatment, intracellular *intI*1 and 16S rDNA decreased by 0.99 and 1.01 log copies, and extracellular *intI*1 and 16S rDNA increased by 1.43 and 2.04 log copies, respectively. Table 1 shows that the abundance of seven ARGs had significant correlations with *intI*1 and 16S rDNA, and the previous study observed that the abundance of ARGs showed positive correlations with *intI*1 (Mao *et al.* 2015). The *intI*1 was one of the main mobile gene elements of ARGs during horizontal gene transfer (Partridge *et al.* 2009). In order to reduce the dissemination risk of ARGs, it was necessary to control the abundance of *intI*1 effectively.

Supplementary material, Figure S4 shows that iARGs are transformed into eARGs as the degree of sludge cracking. The abundance of eARGs was the highest when TAP was conducted for 40 min, and the abundance of eARGs remained stable after 40 min of the TAP. TAP has a significant effect on bacterial disintegration (Zhong *et al.* 2015), and a large amount of eARGs and EPSs was produced after the TAP (Wei *et al.* 2020). The removal efficiency of eARGs was ineffective during the TAP because of the recovery of bacterial DNA (Suss *et al.* 2009). The study shows that the total removal efficiency of ARGs could be improved to 52.50% using alkaline and thermal pretreatment (Wang *et al.* 2019).

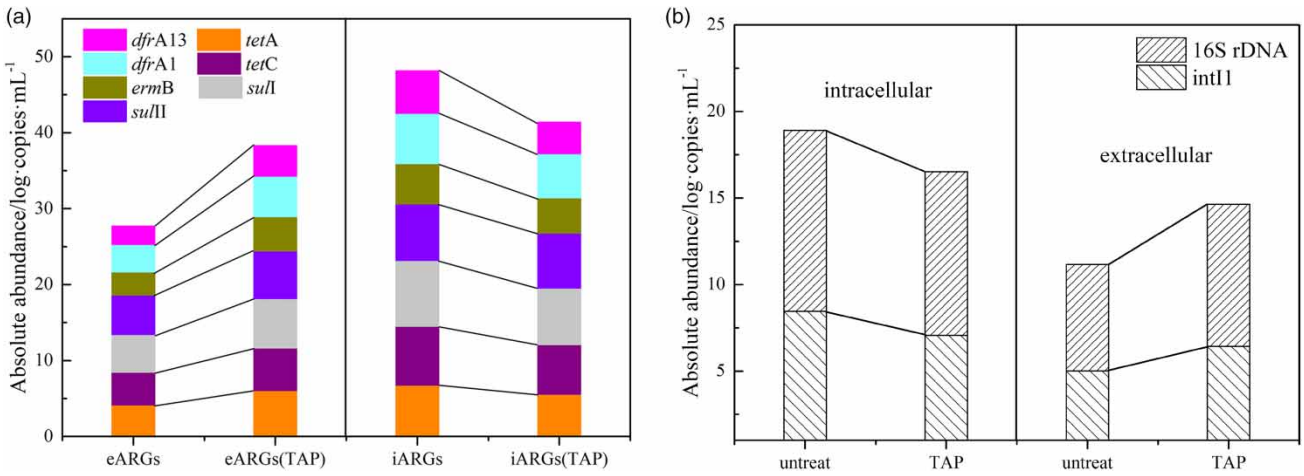

Figure 2 | Absolute abundances of eARGs, iARGs, *intI*1, and 16S rDNA in sludge conditioned with TAP. (a) Abundances of eARGs and iARGs in sludge conditioned with TAP. (b) The abundance of *intI*1 and 16S rDNA (intracellular and extracellular).

Table 1 | Spearman correlations between ARGs and *intI*1 or 16S rDNA

	tetA	***tetC***	***sulI***	***sulII***	***ermB***	***dfrA1***	***dfrA13***
*intI*1	0.932***	0.884***	0.817**	0.705*	0.801**	0.930***	0.840**
16S rDNA	0.849***	0.847**	0.735*	0.752*	0.882***	0.806**	0.949***

*$P < 0.05$.
**$P < 0.01$.
***$P < 0.001$.

3.3. Application of thermal/PS to reduce eARGs

3.3.1. The fate of eARGs, intI1, and 16S rDNA during thermal/PS

Figure 3 shows the abundance of eARGs, *intI*1, and 16S rDNA in the untreated filtrate and thermal/PS process (pH = 7, PS concentration was 0.03 M, the reaction temperature was 80 °C). The abundance of eARGs in untreated filtrate ranged from 9.22×10^3 to 3.24×10^6 copies/mL, and the abundance of *intI*1 and 16S rDNA were 2.67×10^6 and 1.61×10^8 copies/mL, respectively. Thermal/PS could effectively degrade various eARGs. Even the abundance of *dfrA*1 and *dfrA*13 was reduced to the detection limit (<1 copies/mL). It was found that the effect of thermal/PS on eARGs, *intI*1, and 16S rDNA was effective. The *intI*1 was reduced significantly after thermal/PS, indicating a smaller chance of horizontal gene transfer (Pei *et al.* 2016).

3.3.2. Respective roles of pH, PS concentration, and reaction temperature in degrading intI1 during thermal/PS treatment

Different pH values of the filtrate were adjusted for *intI*1 degradation, and the effect is explored in Figure 4. The kinetics of the removal effect could be represented by the fractional-order kinetics model:

$$r = \frac{r_{\max} c + c_0}{k_s + c} \tag{6}$$

where r is the removal rate of *intI*1, c is the concentration of PS, $r_{\max}$ is the maximum removal rate of *intI*1, and c_0 is the initial and available PS concentration.

Table 2 summarizes the $r_{\max}$, k_s, and c_0 parameters derived from experimental data, and Figure 4 plots the fitting curve using Equation (6). The fitting curves were excellent and with Pearson's R^2 value of 0.999 for pH 3, 0.997 for pH 7, and 0.993 for pH 11.

To gain further insight into the effects of pH on the *intI*1 degradation, pH values of 3, 7, and 11 were investigated. Figure 4 shows that the removal efficiency of *intI*1 at pH 11 was significantly better than at pH 3 and pH 7, which was consistent with previous reports (Liu *et al.* 2015; Varanasi *et al.* 2018). It confirmed that the removal efficiency of *intI*1 was dependent on pH, and higher pH could increase the reactivity of PS. The decomposition products of PS were different at various pH conditions (Gao *et al.* 2020). Equations (7) and (8) indicate the decomposition of PS under alkaline conditions (Chen *et al.* 2017). During thermal-activated PS oxidation, PS was photolyzed into $^{\cdot}SO_4^-$ (Equation (7)), which reacts with OH^- and generates $^{\cdot}OH$ (Equation (8)). $^{\cdot}OH$ radicals react with OH^- to generate O^- according to Equation (9) (Varanasi *et al.* 2018), which reduces the concentration of $^{\cdot}OH$. Equations (10) and (11) indicate the decomposition of PS under acidic conditions (Zrinyi & Pham

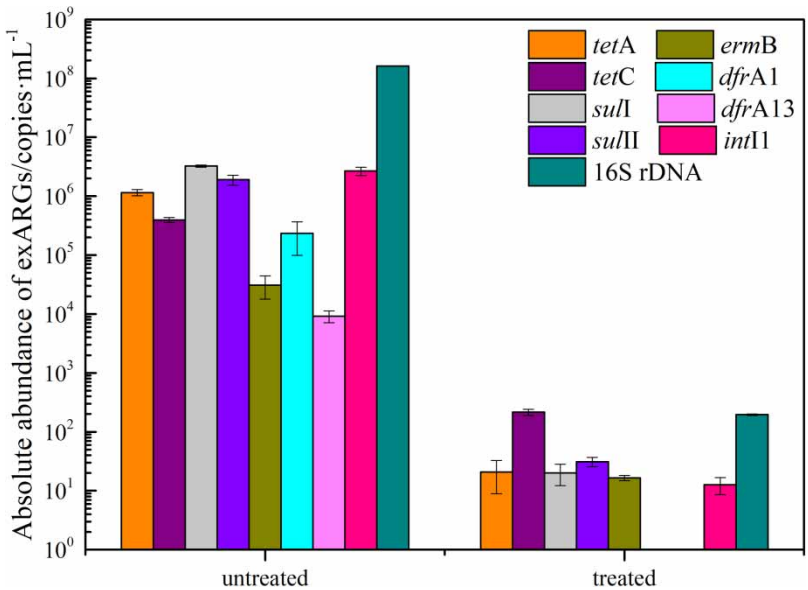

Figure 3 | The abundance of eARGs, *intI*1, and 16S rDNA.

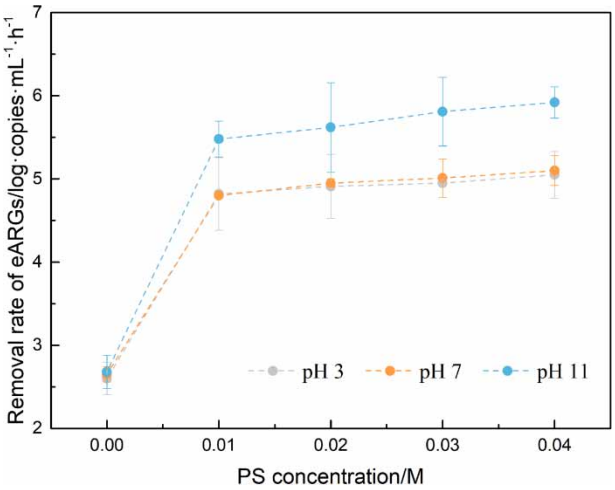

Figure 4 | Experimental removal rate and calculated removal rates for *intI*1 (temperature was kept at 80 °C).

Table 2 | Best-fit parameters r_{max}, k_s, and c_0 for Equation (6)

	r_{max}	k_s	c_0
pH 3	5.343	0.002	0.004
pH 7	5.717	0.004	0.011
pH 11	6.089	0.002	0.005

2017). PS also react with H^+ to generate $^{\cdot}SO_4^-$, and $^{\cdot}SO_4^-$and $^{\cdot}OH$ were considered to be the main oxidizing radical during thermal-activated PS oxidation (Matzek & Carter 2016).

$$S_2O_8^{2-} \rightarrow 2\,{}^{\cdot}SO_4^- \quad (7)$$

$$^{\cdot}SO_4^- + OH^- \rightarrow {}^{\cdot}OH + SO_4^{2-} \quad (8)$$

$$^{\cdot}OH + OH^- \rightarrow H_2O + O^- \quad (9)$$

$$S_2O_8^{2-} + H^+ \rightarrow HS_2O_8^- \quad (10)$$

$$HS_2O_8^- \rightarrow {}^{\cdot}SO_4^- + SO_4^{2-} + H^+ \quad (11)$$

When pH and reaction temperature were stable, *intI*1 removal efficiency increased with PS concentration. It was caused by the increasing oxidizing radical concentration by increasing PS concentration, and oxidizing radicals were directly related to the degradation of *intI*1. A significance relationship was observed between the *intI*1 removal efficiency and the initial PS concentration (Hu *et al.* 2020). When the concentration of PS was higher than 0.01 M, the removal rate of *intI*1 remained stable with the concentration increases.

3.3.3. Determination of the optimal conditions

Figure 5 shows that the removal efficiency of eARGs increased with temperature. When the reaction temperature exceeded 80 °C, the removal efficiency of eARGs decreased with temperature. When pH and temperature were stable, removal efficiency of eARGs increased with PS concentration. It was caused by the increasing oxidizing radical concentration, and oxidizing radicals were directly related to the degradation of eARGs.

Figure 5 indicates that the effect of PS concentration changes on removal was more critical than others. The optimum process parameters for the removal efficiency of *sulI* and *tetA* (pH = 10.24 and 10.22, the temperature was 75.56 and 78.94 °C, PS concentration was 0.038 and 0.040 mg/L) were obtained and their removal efficiency were 6.30 and 6.48 log·copies/mL, respectively.

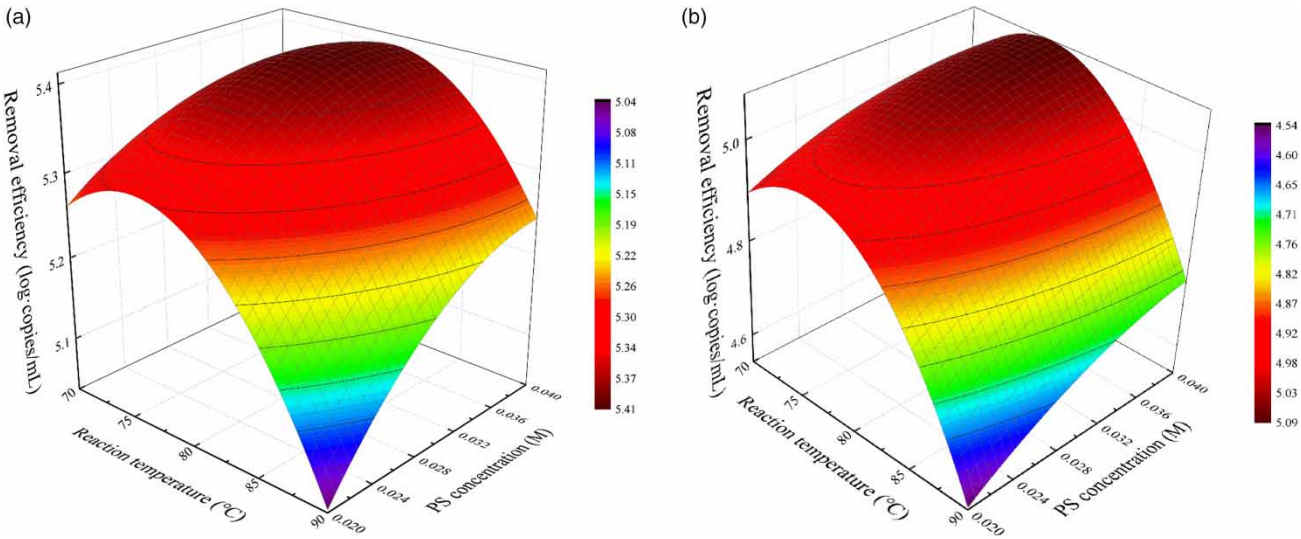

Figure 5 | Three-dimensional surface plots of the experimental data of ARGs removal efficiency by thermal/PS with two shown variables: (a) three-dimensional surface plots of *tetA* removal efficiency and (b) three-dimensional surface plots of *sulI* removal efficiency.

3.3.4. Desirability function

The three-dimensional response surface curves were used to further analyze the interactions between three parameters and their optimal level in the removal efficiency of ARGs (Figure 5). The desirability function is a useful technique in which the maximum removal efficiencies of multiple ARGs need to be optimized simultaneously. The completely desirable and undesirable values of the removal efficiencies of both *tetA* and *sulI* are 7 and 2 log·copies/mL, respectively. The response surface of the desirability value is illustrated in Figure 6. The relatively large curvature of the contour curve shows that the influence of pH and PS concentration on the desirability value is significant. The removal efficiencies of *tetA* and *sulI* were 6.28 and

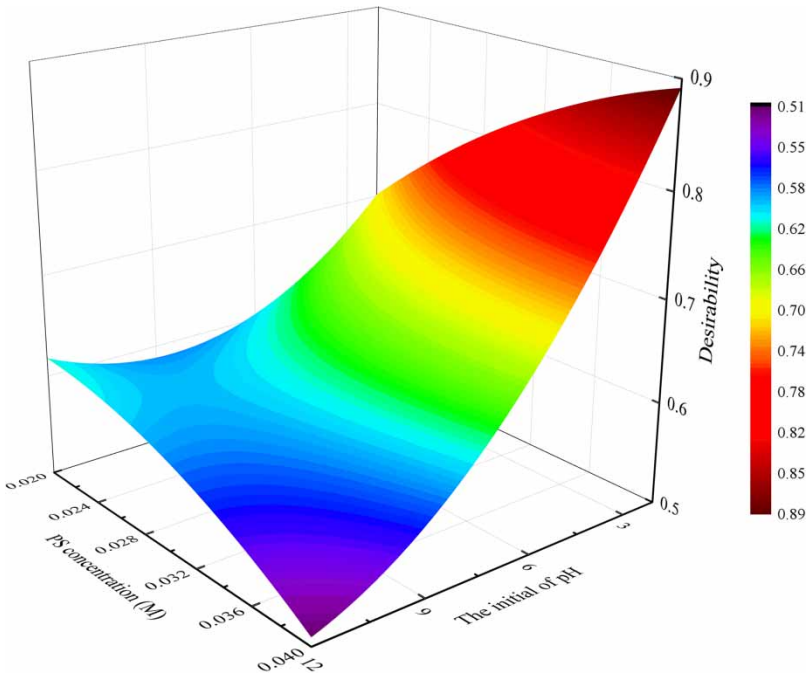

Figure 6 | Three-dimensional surface plots of the desirability function.

6.57 log·copies/mL when the conditions of the independent variable are 10.2 (pH), 75.12 °C (temperature), and 0.039 M (concentration), respectively.

It was notable that the removal efficiency of eARGs in this study was much more significant than in previous studies. For example, Ahmed *et al.* (2020) reported that the photo-Fenton process with conditions of 0.5 mM of Fe^{2+} (2.8 mg/L) and 10 mM of H_2O_2 (170.7 mg/L) would decrease in 6.0 log of eARGs. Yoon *et al.* (2017) used a thermal/H_2O_2 process under the conditions of 60–90 mJ/cm^2 of thermal fluence with 10 mg/L of H_2O_2 that could degrade 4.5 logs of eARGs at pH 7. Compared with previous studies, thermal/PS in this study was more promising than the photo-Fenton process and thermal/H_2O_2 for the removal of eARGs. The higher degradation efficiency of eARGs might be due to the strong oxidation of PS.

4. CONCLUSION

The present study focused on the optimization of the dewatering process, while the fate of eARGs during the TAP and thermal/PS process was also examined. TAP and thermal/PS were proved to be effective for the dewatering of sludge and removal of eARGs in the filtrate, respectively. The main conclusions are given as follows.

The TAP was found to be efficient in dewatering and resulted in the increase in eARGs in the filtrate. The optimal TAP condition for the dewatering rate was obtained by the RSM. The dewatering rate under optimized conditions (pH: 11.2, T: 88 °C, time: 90 min) was 41%. The absolute abundances of eARGs in sludge using TAP increased by 1.06–1.90 log·copies.

The application of thermal/PS as a post-treatment of the TAP was found to be capable of eliminating eARGs in the filtrate. The removal efficiencies of *tetA* and *sulI* under optimized conditions (pH: 10.2, conc.: 0.039 M, temp.: 75.12 °C) were 6.28 and 6.57 log·copies/mL, respectively.

ACKNOWLEDGEMENTS

This study was supported by the project (No. 51678003) granted by the National Natural Science Foundation of China, project (No. 2022C02038) granted by the Science and Technology Project of Zhejiang Province, and project (No. RC2224) granted by the Science and Technology Planning Project of Zhejiang Water Resources Department.

DATA AVAILABILITY STATEMENT

All relevant data are included in the paper or its Supplementary Information.

CONFLICT OF INTEREST

The authors declare there is no conflict.

REFERENCES

Ahmed, Y., Lu, J., Yuan, Z. G., Bond, P. L. & Guo, J. H. 2020 Efficient inactivation of antibiotic resistant bacteria and antibiotic resistance genes by photo-Fenton process under visible LED light and neutral pH. *Water Research* **179**, 14. https://doi.org/10.1016/j.watres.2020.115878.

Asaithambi, P., Alemayehu, E., Sajjadi, B. & Aziz, A. R. A. 2017 Electrical energy per order determination for the removal pollutant from industrial wastewater using UV/Fe^{2+}/H_2O_2 process: optimization by response surface methodology. *Water Resources and Industry* **18**, 17–32. https://doi.org/10.1016/j.wri.2017.06.002.

Bai, Y. H., Sun, Q. H., Wen, D. H. & Tang, X. Y. 2012 Abundance of ammonia-oxidizing bacteria and archaea in industrial and domestic wastewater treatment systems. *Fems Microbiology Ecology* **80** (2), 323–330. https://doi.org/10.1111/j.1574-6941.2012.01296.x.

Bezerra, M. A., Santelli, R. E., Oliveira, E. P., Villar, L. S. & Escaleira, L. A. 2008 Response surface methodology (RSM) as a tool for optimization in analytical chemistry. *Talanta* **76** (5), 965–977. https://doi.org/10.1016/j.talanta.2008.05.019.

Bezerra, M. A., Ferreira, S. L. C., Novaes, C. G., Dos Santos, A. M. P., Valasques, G. S., Cerqueira, U. & Alves, J. P. D. 2019 Simultaneous optimization of multiple responses and its application in analytical chemistry – a review. *Talanta* **194**, 941–959. https://doi.org/10.1016/j.talanta.2018.10.088.

Blokesch, M. 2016 Natural competence for transformation. *Current Biology* **26** (21), R1126–R1130. https://doi.org/10.1016/j.cub.2016.08.058.

Campo, G., Cerutti, A., Zanetti, M., Scibilia, G., Lorenzi, E. & Ruffino, B. 2018 Enhancement of waste activated sludge (WAS) anaerobic digestion by means of pre- and intermediate treatments. Technical and economic analysis at a full-scale WWTP. *Journal of Environmental Management* **216**, 372–382. https://doi.org/10.1016/j.jenvman.2017.05.025.

Chen, Y. Q., Deng, P. Y., Xie, P. C., Shang, R., Wang, Z. P. & Wang, S. L. 2017 Heat-activated persulfate oxidation of methyl- and ethyl-parabens: effect, kinetics, and mechanism. *Chemosphere* **168**, 1628–1636. https://doi.org/10.1016/j.chemosphere.2016.11.143.

Duan, W. J., Gao, J. F., Zhang, W. Z., Wang, Y. W. & Liu, J. 2020 Elimination of antibiotic resistance genes in waste activated sludge by persulfate treatment during the process of sludge dewatering. *Bioresource Technology* **311**, 12. https://doi.org/10.1016/j.biortech.2020.123509.

Furman, O. S., Teel, A. L. & Watts, R. J. 2010 Mechanism of base activation of persulfate. *Environmental Science & Technology* **44** (16), 6423–6428. https://doi.org/10.1021/es1013714.

Gao, J. F., Duan, W. J., Zhang, W. Z. & Wu, Z. L. 2020 Effects of persulfate treatment on antibiotic resistance genes abundance and the bacterial community in secondary effluent. *Chemical Engineering Journal* **382**, 11. https://doi.org/10.1016/j.cej.2019.05.221.

Guo, H. G., Du, L. Z., Liang, J. F., Yang, Z. J., Cui, G. H. & Zhang, K. Q. 2017 Influence of alkaline-thermal pretreatment on high-solids anaerobic digestion of dewatered activated sludge. *Bioresources* **12** (1), 195–210. https://doi.org/10.15376/biores.12.1.195-210.

Hilles, A. H., Abu Amr, S. S., Hussein, R. A., El-Sebaie, O. D. & Arafa, A. I. 2016 Performance of combined sodium persulfate/H_2O_2 based advanced oxidation process in stabilized landfill leachate treatment. *Journal of Environmental Management* **166**, 493–498. https://doi.org/10.1016/j.jenvman.2015.10.051.

Hu, C. Y., Hou, Y. Z., Lin, Y. L., Deng, Y. G., Hua, S. J., Du, Y. F., Chen, C. W. & Wu, C. H. 2020 Investigation of iohexol degradation kinetics by using heat-activated persulfate. *Chemical Engineering Journal* **379**, 11. https://doi.org/10.1016/j.cej.2019.122403.

Inayat, A., Inayat, M., Shahbaz, M., Sulaiman, S. A., Raza, M. & Yusup, S. 2020 Parametric analysis and optimization for the catalytic air gasification of palm kernel shell using coal bottom ash as catalyst. *Renewable Energy* **145**, 671–681. https://doi.org/10.1016/j.renene.2019.06.104.

Khan, S., Naushad, M., Govarthanan, M., Iqbal, J. & Alfadul, S. M. 2022 Emerging contaminants of high concern for the environment: current trends and future research. *Environmental Research* **207**, 112609. https://doi.org/10.1016/j.envres.2021.112609.

Krzeminski, P., Feys, E., D'auriac, M. A., Wennberg, A. C., Umar, M., Schwermer, C. U. & Uhl, W. 2020 Combined membrane filtration and 265 nm UV irradiation for effective removal of cell free antibiotic resistance genes from feed water and concentrate. *Journal of Membrane Science* **598**, 11. https://doi.org/10.1016/j.memsci.2019.117676.

Li, Z. H. & Liu, H. L. 2015 Integrating preference by means of desirability function with evolutionary multi-objective optimization. *Intelligent Automation and Soft Computing* **21** (2), 197–209. https://doi.org/10.1080/10798587.2014.961313.

Li, Z. X., Zuo, J. N., Tian, B. K., Yang, J. L., Yu, X., Chen, P. & Zhao, Y. Q. 2012 Thermal-alkaline pretreatment on the decomposition of the streptomycin bacterial residue. *Biotechnology & Biotechnological Equipment* **26** (3), 2971–2975. https://doi.org/10.5504/bbeq.2012.0042.

Li, G. X., Zhong, W. Z., Wang, R., Chen, J. Q. & Li, Z. X. 2017 Anaerobic digestion of thermal-alkaline-pretreated cephalosporin bacterial residues for methane production. *Journal of the Air & Waste Management Association* **67** (8), 933–937. https://doi.org/10.1080/10962247.2017.1308447.

Liu, N., Sijak, S., Zheng, M., Tang, L., Xu, G. & Wu, M. H. 2015 Aquatic photolysis of florfenicol and thiamphenicol under direct UV irradiation, UV/H_2O_2 and UV/Fe(II) processes. *Chemical Engineering Journal* **260**, 826–834. https://doi.org/10.1016/j.cej.2014.09.055.

Lu, Y., Zhang, C. M., Zheng, G. Y. & Zhou, L. X. 2019 Improving the compression dewatering of sewage sludge through bioacidification conditioning driven by Acidithiobacillus ferrooxidans: dewatering rate vs. dewatering extent. *Environmental Technology* **40** (24), 3176–3189. https://doi.org/10.1080/09593330.2018.1465129.

Lu, J., Wang, Y., Zhang, S., Bond, P., Yuan, Z. G. & Guo, J. H. 2020a Triclosan at environmental concentrations can enhance the spread of extracellular antibiotic resistance genes through transformation. *Science of the Total Environment* **713**, 9. https://doi.org/10.1016/j.scitotenv.2020.136621.

Lu, Y., Xiao, Y. F., Zheng, G. Y., Lu, J. H. & Zhou, L. X. 2020b Conditioning with zero-valent iron or Fe^{2+} activated peroxydisulfate at an acidic initial sludge pH removed intracellular antibiotic resistance genes but increased extracellular antibiotic resistance genes in sewage sludge. *Journal of Hazardous Materials* **386**, 10. https://doi.org/10.1016/j.jhazmat.2019.121982.

Mancuso, G., Langone, M., Andreottola, G. & Bruni, L. 2019 Effects of hydrodynamic cavitation, low-level thermal and low-level alkaline pre-treatments on sludge solubilisation. *Ultrasonics Sonochemistry* **59**, 11. https://doi.org/10.1016/j.ultsonch.2019.104750.

Mao, D. Q., Yu, S., Rysz, M., Luo, Y., Yang, F. X., Li, F. X., Hou, J., Mu, Q. H. & Alvarez, P. J. J. 2015 Prevalence and proliferation of antibiotic resistance genes in two municipal wastewater treatment plants. *Water Research* **85**, 458–466. https://doi.org/10.1016/j.watres.2015.09.010.

Matzek, L. W. & Carter, K. E. 2016 Activated persulfate for organic chemical degradation: a review. *Chemosphere* **151**, 178–188. https://doi.org/10.1016/j.chemosphere.2016.02.055.

Michael-Kordatou, I., Karaolia, P. & Fatta-Kassinos, D. 2018 The role of operating parameters and oxidative damage mechanisms of advanced chemical oxidation processes in the combat against antibiotic-resistant bacteria and resistance genes present in urban wastewater. *Water Research* **129**, 208–230. https://doi.org/10.1016/j.watres.2017.10.007.

Partridge, S. R., Tsafnat, G., Coiera, E. & Iredell, J. R. 2009 Gene cassettes and cassette arrays in mobile resistance integrons. *Fems Microbiology Reviews* **33** (4), 757–784. https://doi.org/10.1111/j.1574-6976.2009.00175.x.

Pei, J., Yao, H., Wang, H., Ren, J. & Yu, X. H. 2016 Comparison of ozone and thermal hydrolysis combined with anaerobic digestion for municipal and pharmaceutical waste sludge with tetracycline resistance genes. *Water Research* **99**, 122–128. https://doi.org/10.1016/j.watres.2016.04.058.

Penghe, Z., Yuling, L., Chuanchuan, D. & Pengliang, W. 2020 Study on dissolution characteristics of excess sludge by low-temperature thermal hydrolysis and acid production by fermentation. *ACS Omega* **5** (40), 26101–26109. https://doi.org/10.1021/acsomega.0c03606.

Pourehie, O. & Saien, J. 2019 Treatment of real petroleum refinery wastewater with alternative ferrous-assisted UV/persulfate homogeneous processes. *Desalination and Water Treatment* **142**, 140–147. https://doi.org/10.5004/dwt.2019.23506.

Pruden, A., Pei, R. T., Storteboom, H. & Carlson, K. H. 2006 Antibiotic resistance genes as emerging contaminants: studies in northern Colorado. *Environmental Science & Technology* **40** (23), 7445–7450. https://doi.org/10.1021/es060413l.

Raheem, A., Ji, G., Memon, A., Sivasangar, S., Wang, W., Zhao, M. & Aufiq-Yap, Y. H. 2018 Catalytic gasification of algal biomass for hydrogen-rich gas production: parametric optimization via central composite design. *Energy Conversion and Management* **158**, 235–245. https://doi.org/10.1016/j.enconman.2017.12.041.

Ran, G. & Li, Q. B. 2020 Degradation of refractory organic compounds from dinitrodiazophenol containing industrial wastewater through UV/H_2O_2 and UV/PS processes. *Environmental Science and Pollution Research* **27** (6), 6042–6051. https://doi.org/10.1007/s11356-019-07367-1.

Ruiz-Hernando, M., Martin-Diaz, J., Labanda, J., Mata-Alvarez, J., Llorens, J., Lucena, F. & Astals, S. 2014 Effect of ultrasound, low-temperature thermal and alkali pre-treatments on waste activated sludge rheology, hygienization and methane potential. *Water Research* **61**, 119–129. https://doi.org/10.1016/j.watres.2014.05.012.

Shahbaz, M., Yusup, S., Inayat, A., Patrick, D. O., Pratama, A. & Ammar, M. 2017 Optimization of hydrogen and syngas production from PKS gasification by using coal bottom ash. *Bioresource Technology* **241**, 284–295. https://doi.org/10.1016/j.biortech.2017.05.119.

Su, S. S., Cao, C. J., Zhao, Y. P. & Dionysiou, D. D. 2019 Efficient transformation and elimination of roxarsone and its metabolites by a new alpha-FeOOH@GCA activating persulfate system under UV irradiation with subsequent As(V) recovery. *Applied Catalysis B-Environmental* **245**, 207–219. https://doi.org/10.1016/j.apcatb.2018.12.050.

Suss, J., Volz, S., Obst, U. & Schwartz, T. 2009 Application of a molecular biology concept for the detection of DNA damage and repair during UV disinfection. *Water Research* **43** (15), 3705–3716. https://doi.org/10.1016/j.watres.2009.05.048.

Toutian, V., Barjenbruch, M., Loderer, C. & Remy, C. 2020a Pilot study of thermal alkaline pretreatment of waste activated sludge: seasonal effects on anaerobic digestion and impact on dewaterability and refractory COD. *Water Research* **182**, 115910. https://doi.org/10.1016/j.watres.2020.115910.

Toutian, V., Barjenbruch, M., Unger, T., Loderer, C. & Remy, C. 2020b Effect of temperature on biogas yield increase and formation of refractory COD during thermal hydrolysis of waste activated sludge. *Water Research* **171**, 11. https://doi.org/10.1016/j.watres.2019.115383.

Tsapekos, P., Kougias, P. G.,, Frison, A., Rage, R. & Angelidaki, I. 2016 Improving methane production from digested manure biofibers by mechanical and thermal alkaline pretreatment. *Bioresource Technology* **216**, 545–552. https://doi.org/10.1016/j.biortech.2016.05.117.

Varanasi, L., Coscarelli, E., Khaksari, M., Mazzoleni, L. R. & Minakata, D. 2018 Transformations of dissolved organic matter induced by UV photolysis, hydroxyl radicals, chlorine radicals, and sulfate radicals in aqueous-phase UV-Based advanced oxidation processes. *Water Research* **135**, 22–30. https://doi.org/10.1016/j.watres.2018.02.015.

Wang, M. L., Li, R. Y. & Zhao, Q. 2019 Distribution and removal of antibiotic resistance genes during anaerobic sludge digestion with alkaline, thermal hydrolysis and ultrasonic pretreatments. *Frontiers of Environmental Science & Engineering* **13** (3), 10. https://doi.org/10.1007/s11783-019-1127-2.

Wei, L. L., Xia, X. H., Zhu, F. Y., Li, Q. Y., Xue, M., Li, J. J., Sun, B., Jiang, J. Q. & Zhao, Q. L. 2020 Dewatering efficiency of sewage sludge during Fe2 + -activated persulfate oxidation: effect of hydrophobic hydrophilic properties of sludge EPS. *Water Research* **181**, 12. https://doi.org/10.1016/j.watres.2020.115903.

Xie, Y. W., Chen, L. J. & Liu, R. 2016 Oxidation of AOX and organic compounds in pharmaceutical wastewater in RSM-optimized-Fenton system. *Chemosphere* **155**, 217–224. https://doi.org/10.1016/j.chemosphere.2016.04.057.

Yoon, Y., Chung, H. J., Di, D. Y. W., Dodd, M. C., Hur, H. G. & Lee, Y. 2017 Inactivation efficiency of plasmid-encoded antibiotic resistance genes during water treatment with chlorine, UV, and UV/H2O2. *Water Research* **123**, 783–793. https://doi.org/10.1016/j.watres.2017.06.056.

Yusup, S., Khan, Z., Ahmad, M. M. & Rashidi, N. A. 2014 Optimization of hydrogen production in in-situ catalytic adsorption (ICA) steam gasification based on Response Surface Methodology. *Biomass & Bioenergy* **60**, 98–107. https://doi.org/10.1016/j.biombioe.2013.11.007.

Zhang, Y., Li, A. L., Dai, T. J., Li, F. F., Xie, H., Chen, L. J. & Wen, D. H. 2018 Cell-free DNA: a neglected source for antibiotic resistance genes spreading from WWTPs. *Environmental Science & Technology* **52** (1), 248–257. https://doi.org/10.1021/acs.est.7b04283.

Zhang, X. D., Lu, Y. T., Yao, J., Wu, Y. J., Tran, Q. C. & Vu, Q. V. 2020 Insight into conditioning landfill sludge with ferric chloride and a Fenton reagent: effects on the consolidation properties and advanced dewatering. *Chemosphere* **252**, 13. https://doi.org/10.1016/j.chemosphere.2020.126528.

Zheng, Y., Zhao, J., Xu, F. Q. & Li, Y. B. 2014 Pretreatment of lignocellulosic biomass for enhanced biogas production. *Progress in Energy & Combustion Science* **42** (1), 35–53. https://doi.org/10.1016/j.pecs.2014.01.001.

Zhong, W. Z., Li, G. X., Gao, Y., Li, Z. X., Geng, X. L., Li, Y. B., Yang, J. L. & Zhou, C. H. 2015 Enhanced biogas production from penicillin bacterial residue by thermal-alkaline pretreatment. *Biotechnology & Biotechnological Equipment* **29** (3), 522–529. https://doi.org/10.1080/13102818.2015.1021277.

Zhu, X. B., Tian, J. P., Liu, R. & Chen, L. J. 2011 Optimization of Fenton and electro-Fenton oxidation of biologically treated coking wastewater using response surface methodology. *Separation and Purification Technology* **81** (3), 444–450. https://doi.org/10.1016/j.seppur.2011.08.023.

Zrinyi, N. & Pham, A. L. T. 2017 Oxidation of benzoic acid by heat-activated persulfate: effect of temperature on transformation pathway and product distribution. *Water Research* **120**, 43–51. https://doi.org/10.1016/j.watres.2017.04.066.

First received 10 December 2022; accepted in revised form 15 April 2023. Available online 27 April 2023